Luteolin potentiates low-dose oxaliplatin-induced inhibitory effects on cell proliferation in gastric cancer by inducing G_2/M cell cycle arrest and apoptosis

JUN MA[1,2*], XIAOJIE CHEN[2*], XUEJIE ZHU[2], ZHAOHAI PAN[2], WENJIN HAO[3], DEFANG LI[2], QIUSHENG ZHENG[2,4] and XUEXI TANG[1]

[1]College of Marine Life Sciences, Ocean University of China, Qingdao, Shandong 266003; [2]School of Integrated Traditional Chinese and Western Medicine, Binzhou Medical University, Yantai, Shandong 264003; [3]School of Life Sciences, Nantong University, Nantong, Jiangsu 226000; [4]School of Pharmacy, Shihezi University, Key Laboratory of Xinjiang Endemic Phytomedicine Resources, Ministry of Education, School of Pharmacy, Shihezi, Xinjiang 832002, P.R. China

Received August 8, 2021; Accepted October 13, 2021

DOI: 10.3892/ol.2021.13134

Abstract. Although the reduction of oxaliplatin doses may alleviate deleterious side effects of gastrointestinal and gynecological cancer treatment, it also limits the anticancer therapeutic effects. As a high-efficient and low-priced herbal medicine ingredient, luteolin is an agent with a broad spectrum of anticancer activities and acts as a potential enhancer of therapeutic effects of chemotherapy agents in cancer treatment. This study focused on the antitumor effects and mechanism of combined treatment with luteolin and oxaliplatin on a mouse forestomach carcinoma (MFC) cell line. The study used CCK-8 assay, flow cytometry, Annexin V-FITC/PI double staining assay, reactive oxygen species testing assay, mitochondrial membrane potential testing assay, and western blot assay. The results showed that luteolin and oxaliplatin exerted synergistic effects on inhibiting MFC cell proliferation by inducing G_2/M cell cycle arrest and apoptosis. Inhibiting the tumor necrosis factor receptor-associated protein 1/phosphorylated-extracellular-regulated protein kinases1/2/cell division cycle 25 homolog C/cyclin-dependent kinase-1/cyclin B1 pathway was indispensable to the combined treatment with luteolin and oxaliplatin to induce G_2/M cell cycle arrest. In addition, luteolin increased oxidative stress in MFC cells treated with a low dose of oxaliplatin. The combined therapy damaged mitochondrial membrane potential and regulated BCL-2-associated X protein and B-cell lymphoma 2 protein expression, leading to apoptosis. Findings of the present study suggest that luteolin may be a qualified chemotherapy enhancer to potentiate the anticancer effects of low-dose oxaliplatin in MFC cells. This work provides a theoretical foundation for future research on applications of luteolin in clinical chemotherapy.

Correspondence to: Dr Qiusheng Zheng, School of Integrated Traditional Chinese and Western Medicine, Binzhou Medical University, 346 Guanhai Road, Laishan, Yantai, Shandong 264003, P.R. China
E-mail: zhengqiusheng@bzmc.edu.cn

Dr Xuexi Tang, College of Marine Life Sciences, Ocean University of China, 5 Yushan Road, Shinan, Qingdao, Shandong 266003, P.R. China
E-mail: tangxx@ouc.edu.cn

*Contributed equally

Abbreviations: TRAP1, tumor necrosis factor receptor-associated protein 1; ERK1/2, extracellular-regulated protein kinases1/2; CDC25C, cell division cycle 25 homolog C; CDK1, cyclin-dependent kinase-1; Bax, BCL-2-associated X protein; Bcl-2, B-cell lymphoma 2; MFC, mouse forestomach carcinoma

Key words: apoptosis, G_2/M cell cycle arrest, luteolin, mouse forestomach carcinoma cells, oxaliplatin

Introduction

Cancer is a major health issue across the globe (1,2). Chemotherapy is an important step in the systemic therapy for cancer, especially for metastatic cancer (3,4). Oxaliplatin is one of the platinum-based anticancer chemotherapy drugs approved by the Food and Drug Administration for the treatment of digestive cancer, including gastric and colon cancer (5). Its anticancer effect is attributed to the formation of intra- or inter-strand crosslinks with nuclear DNA, which breaks the double bond of DNA strands, leading to the failure in DNA translation and transcription (6). Oxaliplatin has widely been applied for the treatment of various types of tumors for many years (7). However, one of the limitations associated with platinum-based chemotherapy is the development of dose-limiting toxicities that prevent continuation of the treatment (8). Therefore, there is a need to make improvements in its use in clinical practice. At present, strategies to limit the chemotherapy of toxicity, such as neurotoxicity, include the co-administration of antioxidants, such as thiols, particularly glutathione (GSH), or vitamin E, together with the platinum agent (9). Thus, we were interested to explore whether herbal

medicine might be a feasible add-on to oxaliplatin cancer treatment.

The combined herbal medicine and Western medical treatment has been used in many patients for a long time. Owing to the poor prognosis of some cancer types when treated with Western medicine, many patients prefer the option of herbal medicine as the adjuvant therapy, expecting to enhance therapeutic efficiency, reduce adverse effects, and improve quality of life (10,11). Based on the patient-tailored diagnosis and treatment, such a combined therapy has attracted more attention in the clinical setting. The physical functions were significantly improved in participants with non-small-cell lung cancer treated with the combined herbal-Western medicine than in those treated with Western medicine only (12). In addition, nature-derived products have recently attained a lot of interest due to their potentiation of anticancer effects by modulating the signaling pathways involved in cancer proliferation, and owing to their protective potential in radiotherapy and chemotherapy (13). For example, some *in vitro* and *in vivo* tests confirmed that alteronol, a herbal medicine-extracted ingredient, could potentiate the therapeutic effects of Adriamycin on breast cancer cells and reduce toxicities to major organs in mice (14). Thus, introducing novel bioactive components with natural origins could be considered to treat different types of human cancer on the basis of their selective molecular targets (1).

Luteolin (3',4',5,7-tetrahydroxyflavone) is a natural flavonoid, widely existing in medical plants, such as *Lonicera japonica* Thunb and *Ajuga nipponensis* Makino (1). Luteolin possesses various pharmacological effects, including anticancer, antioxidant, anti-inflammatory, immunoregulatory, and cardioprotective ones (15). Luteolin is compatible with various drugs and enhances their therapeutic effects in the treatment of many diseases, such as Alzheimer disease, diabetic cystopathy, and sciatic nerve ligation-induced neuropathy (16-18). Moreover, luteolin can be utilized as an agent that both improves the therapeutic effects on various types of cancer and decreases toxicity in the host. Furthermore, luteolin is known to effectively act in combination with silibinin (19), sorafenib (20), 5-flurouracil (21), and lycopene (22) against hepatocellular carcinoma cells, glioblastoma cells, ovarian cancer cells, and Solid Ehrlich Carcinoma (SEC). Research on the use of the combined chemotherapy in clinical setting is of even higher interest. Normally, chemotherapeutic drugs exhibit antitumor activities along with deleterious effects, which has been the challenge in the cancer treatment. The dose reduction of these drugs may alleviate their side effects, and it can also limit their efficiency of inhibiting tumor growth (23). Therefore, further studies on potential chemotherapeutic properties of luteolin in cancer treatment are needed, including studies of the underlying mechanism.

In the present study, mouse forestomach carcinoma (MFC) cells were used as the cell model to identify the anticancer effects of the combined treatment with luteolin and oxaliplatin. The MFC cell line with high metastasis is prone to blood-born metastasis to lung. The aim of the present study was to investigate the enhancing effects of luteolin on low-dose oxaliplatin-induced proliferation inhibition in MFC cells. The difference between the combined and monotherapy were demonstrated, supporting the potential of luteolin to enhance the therapeutic effects of oxaliplatin. And this work was also conducted to confirm the key signaling pathway involved in the enhanced effects of the combined treatment with luteolin and oxaliplatin. Therefore, findings of the present study may provide a theoretical foundation for further clinical chemotherapy research on the use of luteolin.

Materials and methods

Reagents. Luteolin (purity, ≥98%) was purchased from Sigma-Aldrich (cat. no. L9283). DMSO (cat. no. D8371; Beijing Solarbio Science & Technology Co., Ltd.) was used to dissolve with luteolin as the mother solution. Oxaliplatin was purchased from Tai-Tianqing Pharmaceutical Co., Ltd. (cat. no. H20143263). Oxaliplatin was dissolved with PBS (P1020; Beijing Solarbio Science & Technology Co., Ltd.). Luteolin and/or oxaliplatin were diluted to the required concentration (luteolin: 10, 20, 30, 40, 50, 60, 70 and 80 μM; and oxaliplatin: 5, 10, 20, 30, 40, 50, 60, 70 and 80 μM) with RPMI-1640 complete medium. RPMI-1640 complete medium (cat. no. 31800; Beijing Solarbio Science & Technology Co., Ltd.) containing 0.1% DMSO was used as a control.

Cell culture. The MFC cell line was purchased from the National Infrastructure of Cell Line Resource (cat. no. 1101MOU-PUMC000143). The cells were cultured with RPMI-1640, containing 10% fetal bovine serum (cat. no. REF10091-48; Gibco; Thermo Fisher Scientific, Inc.), and incubated in an incubator (HF90/HF240; Heal Force) at 5% CO_2 at 37˚C. The cells were treated with different concentrations of luteolin and/or oxaliplatin for 24 h in the subsequent experiments.

CCK-8 cell viability assay and Chou-Talalay combination index (CI) method analysis. The effect of luteolin and/or oxaliplatin on MFC cell viability was determined by CCK-8 assay (24). Briefly, MFC cell suspension (100 μl/well) was seeded at a density of 6,000-7,000 cells/well in a 96-well plate. After incubation for 24 h, the supernatant was discarded, and the cells were treated with luteolin (10, 20, 30, 40, 50, 60, 70, and 80 μM) and oxaliplatin (5, 10, 20, 30, 40, 50, 60, 70, and 80 μM) (total volume 200 μl/well) for 24 h. Based on the CCK-8 cell proliferation and cytotoxicity assay kit (cat. no. CA1210; Beijing Solarbio Science & Technology Co., Ltd.) protocol, 100 μl testing solution (CCK-8: Complete RPMI-1640, 1:10) was added to each well. After incubation at 37˚C in 5% CO_2 in the dark for 1 h, the absorbance at a wavelength of 450 nm was detected via a Thermo 3001 multi-function microplate reader (Infinite 200 PRO; Tecan Austria GmbH). IC_{50} indicated the drug concentration resulted in 50% reduction in cell survival. The Chou-Talalay CI method and Compusyn 2.0 software were used to calculate the CI and the dose reduction index (DRI). The CI was calculated as $(D)_1/(Dx)_1 + (D)_2/(Dx)_2$, where $(Dx)_1$ and $(Dx)_2$ were the doses of drug 1 and 2 alone that inhibit x%, while $(D)_1$ and $(D)_2$ were the portions of drug 1 and 2 in combination to achieve x%. This equation was used to quantitatively depict the synergism (CI <1), additive effect (CI=1), and antagonism (CI >1) (25).

DNA contents analysis. DNA contents analysis was conducted by PI staining and flow cytometry (26). MFC cells were seeded

in a 6-well plate at 2.5x10^5 cells/well and incubated at 37˚C in a 5% CO_2 incubator for 24 h. After treatment with luteolin (20 μM) and/or oxaliplatin (5 μM) (total volume 3 ml/well) for one day, the cells were collected and fixed in 75% ethanol at 4˚C for 4-5 h. In accordance with the manufacturer's instructions of the DNA content quantitation assay kit (cat. no. CA1510; Beijing Solarbio Science & Technology Co., Ltd.), the fixed cells were stained by PI staining solution (50 ng/ml) and RNase A (0.1 mg/ml) at 37˚C in the dark for 30 min. FACSCanto II flow cytometer (BD Biosciences) recorded the DNA content in MFC cells. The data were analyzed by FACSDiva software (version 6.1.3; BD Biosciences).

Hoechst-33258 staining. MFC cells were seeded in a 6-well plate at 2.0x10^5 cells/well. The cells were treated with luteolin (20 μM) and/or oxaliplatin (5 μM) (total volume 3 ml/well) for 24 h. Based on Hoechst-33258 stain solution (cat. no. C0021; Beijing Solarbio Science & Technology Co., Ltd.) instructions (14), the cells were incubated with 500 μl staining working solution at room temperature in the dark for 5 min and soaked in PBS three times for 5 min. Inverted fluorescence microscopy (DMI3000; Leica Microsystems GmbH) was used to detect blue nuclei.

Annexin V-FITC/PI double staining assay. Apoptosis induced by luteolin was examined by fluorescein isothiocyanate (Annexin V-FITC) and propidium iodide (PI) double-staining assay (27). MFC cells were seeded in a 6-well plate at 2.5x10^5 cells/well and incubated at 37˚C in 5% CO_2 for 24 h. The cells were treated with luteolin (20 μM) and/or oxaliplatin (5 μM) (total volume 3 ml/well) for 24 h. After the treatment, the supernatant was discarded. In line with the instructions of the Annexin V-FITC/PI apoptosis detection kit (cat. no. CA1020; Beijing Solarbio Science & Technology Co., Ltd.), the cells were pre-processed and stained using Annexin V-FITC/PI in the dark for 30 min. The fluorescence intensity was measured using FACSCanto II flow cytometer (BD Biosciences), and the apoptotic rates were analyzed using FACSDiva software (version 6.1.3, BD Biosciences).

Reactive oxygen species (ROS) levels testing. Subsequent to the indicated drug treatment for 24 h, the supernatant was discarded. The cells were rinsed with PBS, and stained with 10 μM DCFH-DA solution in the dark for 30 min in accordance with the reactive oxygen species assay kit (cat. no. CA1410; Beijing Solarbio Science & Technology Co., Ltd.) protocol (28). Inverted fluorescence microscopy (DMI3000, Leica) was used to record the morphological changes. The stained cells were analyzed by FACSCanto II flow cytometer (BD Biosciences). The fluorescence mean value in P2 from the flow cytometer was collected using FACSDiva software (version 6.1.3, BD Biosciences), which was used for quantitative analysis. The data were presented as fold increase normalized to the control group.

Measurement of mitochondrial membrane potential (MMP). MMP was measured using a mitochondrial membrane potential assay kit with JC-1 (cat. no. M8650; Beijing Solarbio Science & Technology Co., Ltd.) (29). The treated MFC cells were stained with JC-1 fluorescence working solution in accordance with the protocol. MMP of stained cells was measured by FACSCanto II flow cytometer (BD Biosciences) and analyzed by FACSDiva software (version 6.1.3, BD Biosciences). The relative ratio of P2 (red fluorescence) to P3 (green fluorescence) was used for quantitative analysis of MMP change in MFC cells.

Protein extraction and quantification. A total of 3x10^6 MFC cells were inoculated into 100-mm culture dishes. After overnight culture, the cells were incubated with luteolin (20 μM) and/or oxaliplatin (5 μM) (total volume 7 ml/well) for 24 h. Then, the cells were rinsed with PBS and lysed on ice for 30 min with RIPA buffer (cat. no. R0010; Beijing Solarbio Science & Technology Co., Ltd.) containing 0.1 M PMSF (cat. no. P0100; Beijing Solarbio Science & Technology Co., Ltd.) and protease phosphatase inhibitor (cat. no. P1261; Beijing Solarbio Science & Technology Co., Ltd.). The cell lysate was centrifuged at 12,000 x g (Thermo Scientific™ Sorvall™ Legend™ Micro 21R Microcentrifuge; Thermo Fisher Scientific, Inc.) for 15 min at 4˚C, and the supernatant was collected for the subsequent tests. The protein quantification was performed using the BCA protein assay kit (cat. no. PC0020; Beijing Solarbio Science & Technology Co., Ltd.) (30). The data were obtained at the absorbance of 562 nm by a microplate reader (Infinite 200 PRO, Tecan, Tecan Austria GmbH). The amount of protein was calculated in accordance with the prescribed computational formula of the kit's protocol.

Western blot assay. In total, 50 μg cell lysates from each group were loaded per lane and separated by SDS-PAGE (6% spacer gel and 10% separating gel). Next, cell lysates in the gel were transferred to PVDF membranes (cat. no. ISEQ00010; MilliporeSigma). The transferred membranes were blocked with Tris-buffered saline (10 mM Tris-Cl; pH 7.4), containing 0.5% Tween-20 and 5% skimmed dry milk, at room temperature for 2 h, and then incubated with primary antibodies at 4˚C overnight (31), respectively. The primary antibodies used were: β-actin mouse monoclonal antibody (cat. no. TA-09; 1:2,000; OriGene Technologies, Inc.), Bcl-2 rabbit polyclonal antibody (cat. no. ab196495, 1:1,000; Abcam), BCL-2-associated X protein (Bax) rabbit monoclonal antibody (cat. no. ab182734; 1:1,000; Abcam), cyclin A2 rabbit monoclonal antibody (cat. no. ab181591; 1:2,000; Abcam), cyclin B1 rabbit monoclonal antibody (cat. no. ab32053; 1:1,000; Abcam), cyclin-dependent kinase-1 (CDK1) rabbit monoclonal antibody (cat. no. ab133327; 1:20,000; Abcam), tumor necrosis factor receptor-associated protein 1 (TRAP1) rabbit polyclonal antibody (cat. no. 10325-1-AP; 1:2,000; ProteinTech Group, Inc.), cell division cycle 25 homolog C (CDC25C) mouse monoclonal antibody (cat. no. 66912-1-lg; 1:2,000; ProteinTech Group, Inc.), extracellular-regulated protein kinases1/2 (ERK1/2) rabbit polyclonal antibody (cat. no. 9102s; 1:1,000; Cell Signaling Technology, Inc.) and p-ERK1/2 mouse monoclonal antibody (cat. no. 9106s; 1:1,000; Cell Signaling Technology, Inc.). The membranes were rinsed with TBST and then probed with appropriate secondary antibodies (peroxidase-conjugated goat anti-mouse IgG (H+L); cat. no. ZB-2305; 1:50,000; OriGene Technologies, Inc.; and goat anti-rabbit IgG H&L; ab6721; cat. no. 1:20,000; Abcam). The immunoreactive protein bands were visualized with the gel imaging analysis system (BioSpectrum 510 Imaging System Motorized Platform).

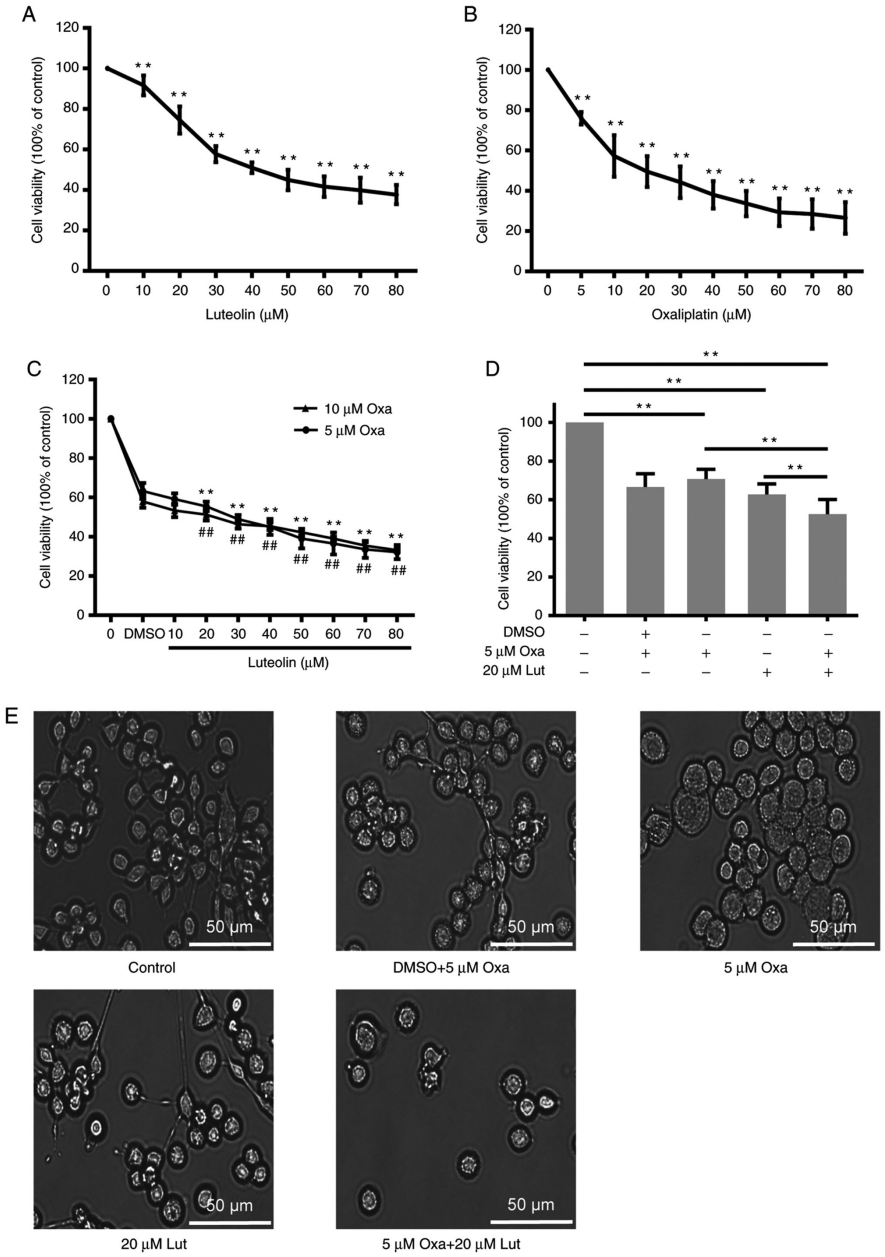

Figure 1. Viability of MFC cells treated with luteolin and/or oxaliplatin. (A) Cell viability induced by a series of doses of luteolin was detected by CCK-8 assay. **P<0.01 vs. 0 group. (B) Cell viability induced by a series of doses of oxaliplatin was detected by CCK-8 assay. 5 μM Oxa: **P<0.01 vs. DMSO group; 10 μM Oxa: $^{\#\#}$P<0.01 vs. DMSO group. (C) The combined effects of a series of doses of luteolin and/or oxaliplatin (5 and 10 μM) were evaluated by CCK-8 assay. **P<0.01 vs. DMSO group. (D) Quantitative analysis of cell viability was performed on MFC cells exposed to luteolin (20 μM) and/or oxaliplatin (5 μM) by using the GraphPad Prism 6.0 software. **P<0.01. (E) The morphological changes were observed under a light microscope (magnification, x200). RPMI-1640 complete medium containing 0.1% DMSO was used as a control. The experiments were repeated ≥3 times. The data are presented as mean ± standard deviation (SD). Lut, luteolin; Oxa, oxaliplatin; MFC, mouse forestomach carcinoma.

Scanning gray analysis was analyzed by Photoshop CC 2019 software (Adobe Systems Inc.). The grayscale value of each band was used to plot histograms.

Statistical analysis. The experiments were performed at least 3 times. Data were analyzed using the SPSS 21.0 software package (version 21.0, SPSS Inc.), and presented as mean ± standard deviation (SD). Scanning gray analysis was calculated by Photoshop CC software (Adobe Systems Inc.) Statistical differences were calculated using ANOVA followed by Tukey's post hoc test. P<0.05 was considered to indicate a statistically significant difference.

Results

Inhibitory effects of luteolin and/or oxaliplatin on MFC cell viability. To investigate the inhibitory effects of luteolin and/or oxaliplatin on mouse forestomach carcinoma MFC cells, CCK-8 assay was performed on MFC cells exposed to a series of luteolin (10, 20, 30, 40, 50, 60, 70, and 80 μM) and oxaliplatin concentrations (5, 10, 20, 30, 40, 50, 60, 70, and 80 μM) for 24 h. Luteolin and oxaliplatin effectively exerted inhibitory effects on MFC cells proliferation in a dose-dependent manner (Fig. 1A and B). Based on the cell viability curve, 50 and 20 μM were calculated as the IC_{50} values of luteolin

Table I. Analysis of luteolin and oxaliplatin[a].

		Combined treatment		Drug alone		DRI	
Fa	CI	Luteolin (μM)	Oxaliplatin (μM)	Luteolin (μM)	Oxaliplatin (μM)	Luteolin	Oxaliplatin
0.403	0.703	10	5	35.080	11.956	3.508	2.391
0.456	0.801	20	5	41.048	15.927	2.052	3.185
0.523	0.821	30	5	49.878	22.729	1.663	4.546
0.580	0.840	40	5	58.967	30.853	1.474	6.171
0.645	0.808	50	5	71.955	44.373	1.439	8.875
0.675	0.851	60	5	79.288	52.973	1.321	10.595
0.697	0.902	70	5	85.389	60.649	1.220	12.130
0.706	0.986	80	5	88.094	64.202	1.101	12.840

[a]Chou-Talalay CI method and Compusyn 2.0 software were used to calculate the CI and the DRI. Fa, effect levels, stands for the efficiency of combined treatment; CI, combination index; DRI, dose reduction index.

and oxaliplatin to MFC cells, respectively. The CI was used to quantitatively depict the synergism (CI <1), additive effect (CI=1), and antagonism (CI >1) in the combined treatment (25). DRI is a measure of how many folds the dose of each drug in a synergistic combination may be reduced at a given effect level when compared with the doses of each drug alone. A greater DRI value indicates a greater dose reduction of the single drug to create the same effect (14). According to the Compusyn analysis in Table I, the CI of luteolin (20 μM) and oxaliplatin (5 μM) was 0.801, suggesting that luteolin and oxaliplatin exerted synergic effects on inhibiting MFC cell proliferation. DRIs for luteolin (20 μM) and oxaliplatin (5 μM) was >1, indicating that the dose reduction led to toxicity reduction in the therapeutic applications (25). The data from CCK-8 assays showed that the combined treatment with luteolin (20 μM) and oxaliplatin (5 μM) exerted a much stronger anticancer effect than the monotherapies (Fig. 1C). Oxaliplatin at 10 μM did not exhibit much stronger inhibitory effects on cell proliferation compared with 5 μM oxaliplatin (Fig. 1D). The morphological change was observed under a light microscope, showing that the cell number was more markedly reduced after the combined treatment than after the monotherapy (Fig. 1E).

G_2/M phase arrest induced by luteolin and/or oxaliplatin in MFC cells. Cell cycle arrest is one of the main causes of the inhibition of cell proliferation (1,32). We examined whether cell cycle arrest had an impact on the combined treatment. MFC cells were treated with luteolin (20 μM) and/or oxaliplatin (5 μM) for 24 h and stained with PI prior to flow cytometry analysis. As shown in Fig. 2A, the combined treatment significantly induced G_2/M phase arrest and exhibited much stronger effects on G_2/M phase arrest than any other single drug did (Fig. 2B). Next, western blotting was used to test the expression levels of the key proteins related to G_2/M phase arrest in the treated MFC cells. The combined therapy of MFC cells markedly reduced the expression levels of cyclin B1, and CDK1 compared with controls and any other monotherapy (Fig. 2C and D). These data indicated that luteolin and oxaliplatin effectively induced MFC cell cycle arrest by downregulating the expression levels of certain key proteins, such as cyclin B1 and CDK1. The combined treatment had significant effects on triggering G_2/M phase arrest ($P<0.01$). Thus, the combined treatment with luteolin and oxaliplatin possibly suppressed cell proliferation via inducing G_2/M phase arrest.

Key signaling protein affected by luteolin and/or oxaliplatin in MFC cells. TRAP1, ERK1/2, and CDC25C are closely related to G_2/M cell cycle arrest and apoptosis (33,34). Thus, the changes in expression levels of TRAP1, P-ERK1/2/ERK1/2, and CDC25C proteins in MFC cells treated with luteolin and/or oxaliplatin as mentioned before were examined by western blot analysis. As shown in Fig. 3, the combined treatment reduced the expression levels of TRAP 1 (Fig. 3A), P-ERK1/2 (Fig. 3B) and CDC25C (Fig. 3C) protein more effectively than the monotherapies. Compared with the control and oxaliplatin group, the combined treatment significantly reduced the TRAP1 and CDC25C proteins expressions ($^*P<0.05$). The combined treatment also significantly downregulated ERK1/2 phosphorylation, thereby suppressing ERK1/2 activation. Thus, the combined treatment with luteolin and oxaliplatin induced G_2/M cell cycle arrest through suppression of TRAP 1/P-ERK1/2/CDC25C in MFC cells.

Apoptosis induced by luteolin and/or oxaliplatin in MFC cells. The artificial regulation of apoptosis remains a considerable focus of attention in cancer treatment (35). Thus, whether apoptosis was involved in anticancer activities of luteolin and/or oxaliplatin was examined. MFC cells were exposed to luteolin (20 μM) and/or oxaliplatin (5 μM), and stained by Hoechst-33258 staining. Images captured from a fluorescence inversion microscope system showed that the combined treatment group manifested a more apparent apoptotic morphology, such as karyopyknosis and chromosome condensation, than other groups (Fig. 4A). By contrast, in the control group, the cells were still in the process of mitosis. The quantitative analysis was used to measure the apoptotic rate by Annexin-V FITC/PI double staining and flow cytometry. The percentage of apoptotic cells in the combined therapy group was much higher than that in the

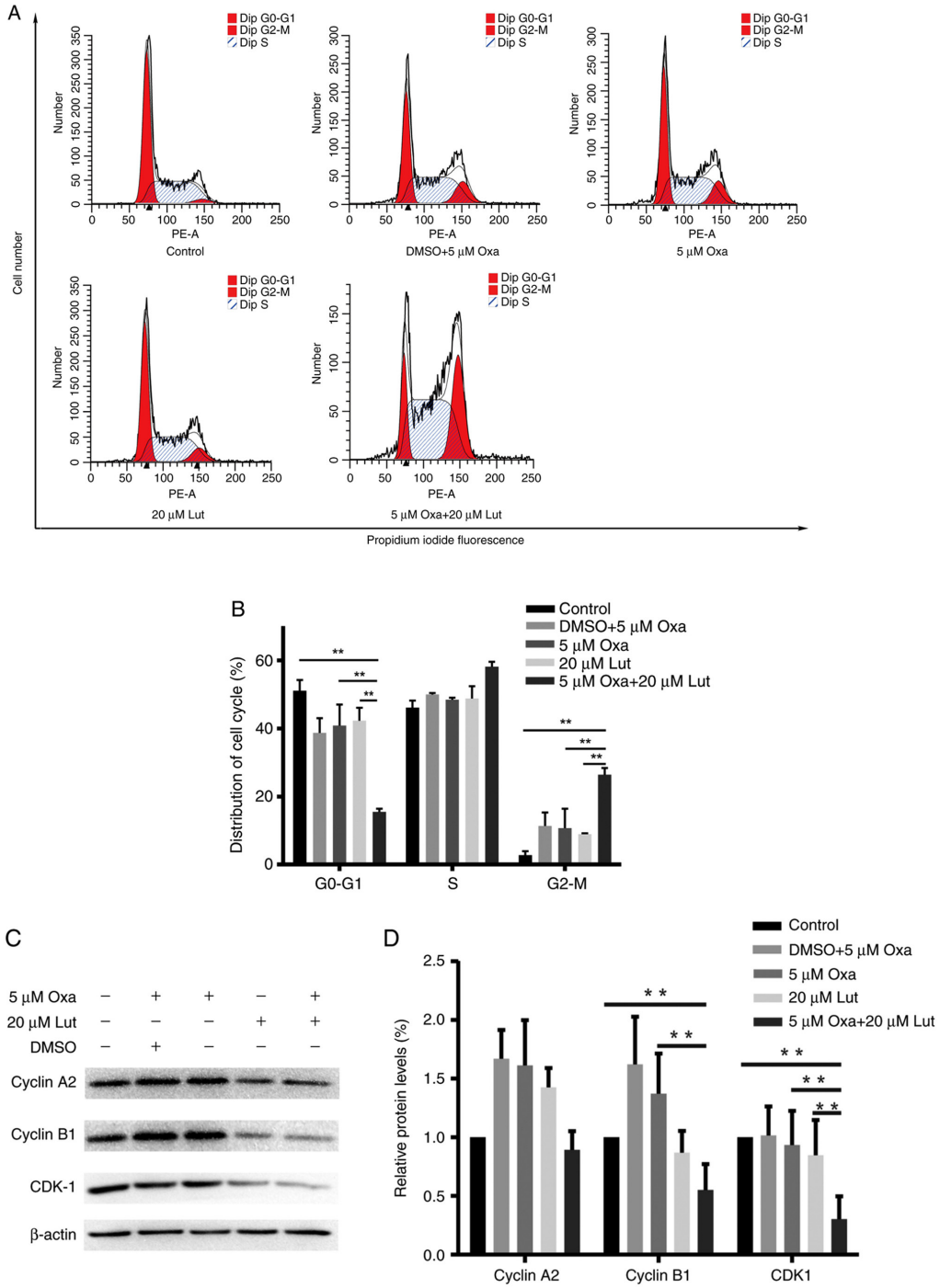

Figure 2. Cell cycle phase change of mouse forestomach carcinoma cells was induced by luteolin (20 μM) and/or oxaliplatin (5 μM). (A and B) Flow cytometry was used to record the cell number on each phase of the cell cycle; the distribution of the cell cycle is shown on the histogram. (C) Cyclin A2, cyclin B1, CDK1 and β-actin expression levels were tested using western blot analysis. (D) Quantitative analysis of cyclin A2, cyclin B1, and CDK1 expression levels relative to β-actin is shown on the histogram. The data were presented as mean ± SD; **P<0.01. The experiments were repeated at least in triplicate. Lut, luteolin; Oxa, oxaliplatin; CDK1, cyclin-dependent kinase-1.

control group (Fig. 4B and C), but for 20 μM luteolin and 5 μM oxaliplatin as monotherapies, the result was not significant compared with the control. Usually, the balance between proapoptotic and antiapoptotic protein regulators is a critical point to determine whether a cell undergoes apoptosis (36). Thus, the protein expression levels of Bcl-2 and Bax were assessed by western blot analysis (Fig. 4D). In accordance with the results of flow cytometry, the ratio of Bcl-2/Bax was markedly lower in the combined group (Fig. 4E). Thus, the combined treatment exerted stronger effects on inducing apoptosis in MFC cells.

ROS and mitochondrial membrane potential influenced by luteolin and/or oxaliplatin in MFC cells. ROS are the primary secondary messengers, and are involved in many biological processes, including apoptosis and cell cycle (37). Therefore, the role of ROS in these processes was examined. DCFH-DA staining and flow cytometry were performed to examine ROS

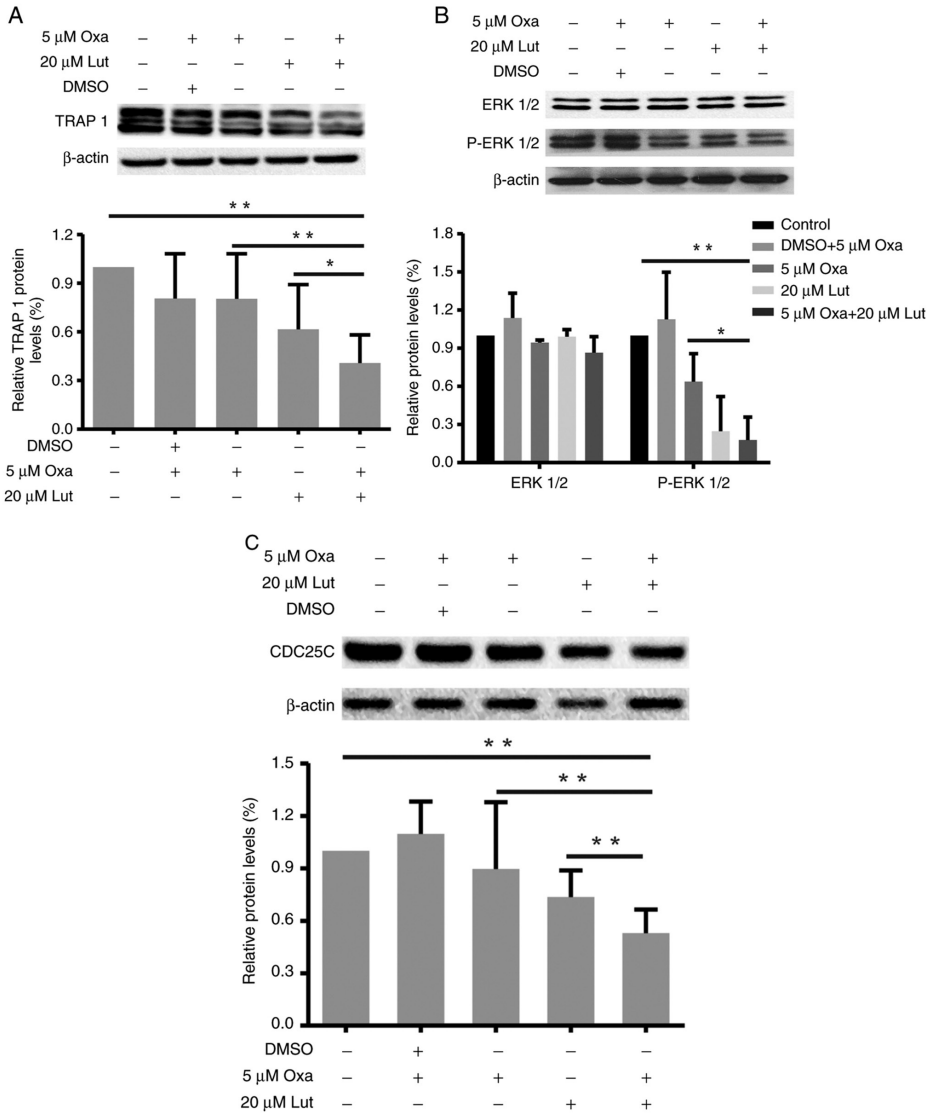

Figure 3. Changes in TRAP1, P-ERK1/2/ERK1/2 and CDC25C protein expression levels in mouse forestomach carcinoma cells induced by luteolin (20 μM) and/or oxaliplatin (5 μM). (A-C) TRAP1, P-ERK1/2/ERK1/2, CDC25C and β-actin protein expression levels were assessed by western blot analysis, and quantitative analysis of protein expression levels is shown in the histogram. *P<0.05, **P<0.01. Experiments were repeated at least in triplicate. Lut, luteolin; Oxa, oxaliplatin; TRAP1, tumor necrosis factor receptor-associated protein 1; ERK1/2, extracellular-regulated protein kinases1/2; CDC25C, cell division cycle 25 homolog C.

accumulation in all of the groups. Based on the fluorescence inversion microscope system, stronger green fluorescence was evident in the combined group than in the other groups (Fig. 5A). The results from the flow cytometry showed that P2 peaks of the drug groups moved to the right compared with the control group, and quantitative analysis verified that the combined treatment was able to more effectively induce ROS accumulation in MFC cells than any monotherapy (Fig. 5B and C). Thus, the combined treatment exerted stronger effects on inducing ROS accumulation in MFC cells. Mitochondria are the main cell organelles where ROS are generated. MMP becomes abnormal when ROS generation exceeds the threshold value, and mitochondrial function is damaged by ROS over-capacity (37). JC-1 fluorescence staining and flow cytometry were applied to examine the MMP change of MFC cells exposed to drug treatments. The results showed that the combined treatment significantly induced MMP reduction, compared with any monotherapy (Fig. 5D and E). Thus, it was suggested that luteolin and oxaliplatin jointly exerted destructive effects on MMP and destroyed mitochondrial function in MFC cells.

Discussion

To verify the enhanced effects of luteolin on efficiency of low-dose oxaliplatin for inhibiting tumor growth, we examined the combined effects of luteolin and oxaliplatin in MFC cells and revealed the underlying mechanism. First of all, the results showed that the combination of luteolin and oxaliplatin significantly inhibited MFC cell proliferation, which was even more effective than any monotherapy. According to the Chou-Talalay method, the CI was much lower than 1, indicating that the combined treatment of luteolin and oxaliplatin exerted synergistic effects on reducing MFC cell viability. Throughout all of the experiments, luteolin did not separate from oxaliplatin solution, suggesting that it had excellent stability and compatibility with oxaliplatin.

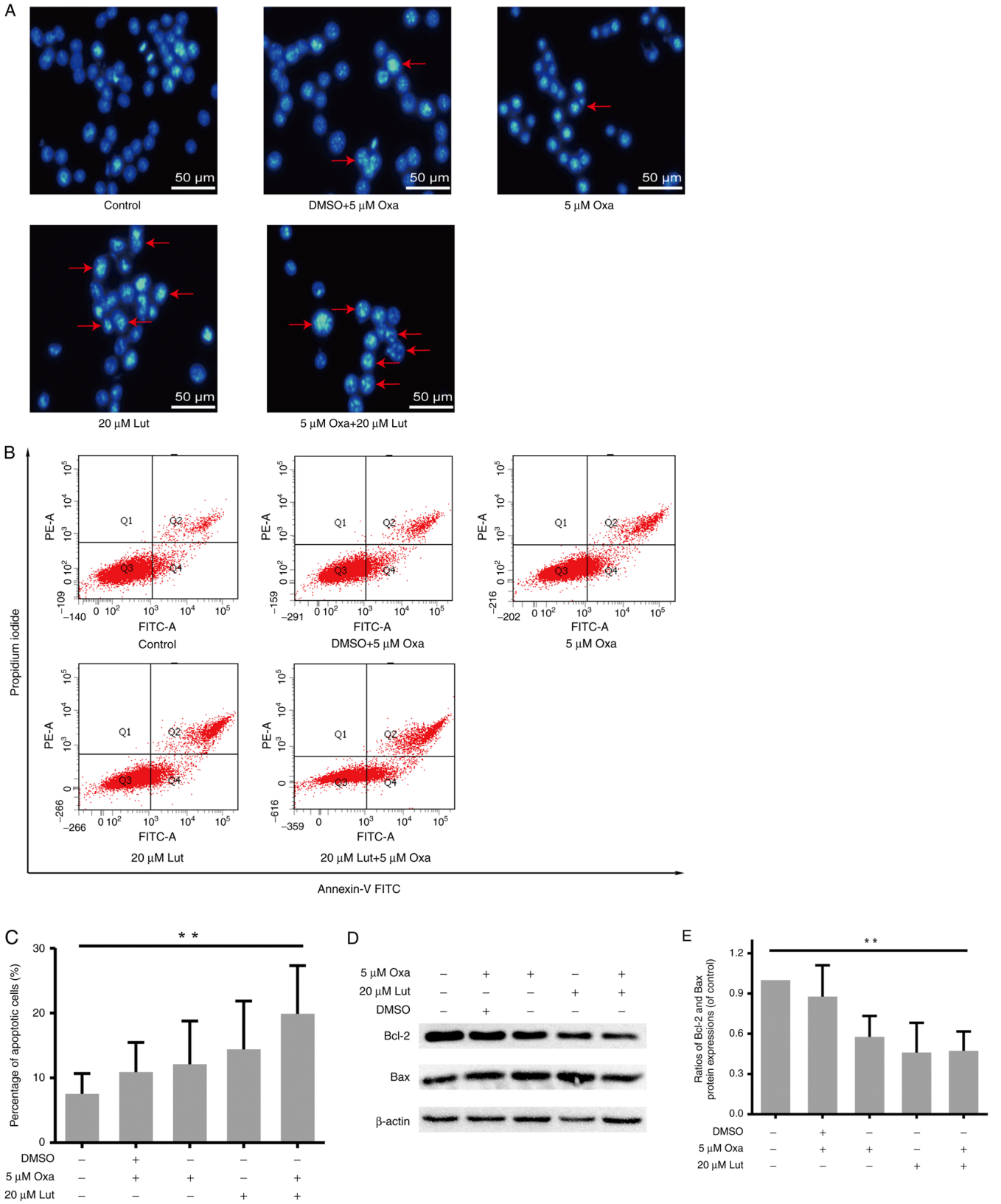

Figure 4. MFC cell apoptosis induced by luteolin (20 μM) and/or oxaliplatin (5 μM). (A) The morphological changes indicative of MFC cell apoptosis were assessed by fluorescence inverted microscopy (magnification, x200). (B and C) After double-staining with Annexin-V FITC and PI, flow cytometry was used for the quantitative analysis of MFC cell apoptosis. (D) Protein expression levels (Bcl-2, Bax, and β-actin) were assessed by western blot analysis. (E) Scanning gray analysis was calculated by Photoshop CC software (Adobe Systems Inc.). Data are presented as mean ± SD, **P<0.01. Experiments were repeated at least 3 times. MFC, mouse forestomach carcinoma; Lut, luteolin; Oxa, oxaliplatin; Bax, BCL-2-associated X protein; Bcl-2, B-cell lymphoma 2.

The next step involved the manner of inhibiting the proliferation. Oxaliplatin, a kind of metal compound, is an alkylating agent extensively applied in the treatment of gastrointestinal and gynecological cancers. The key of its anticancer activity

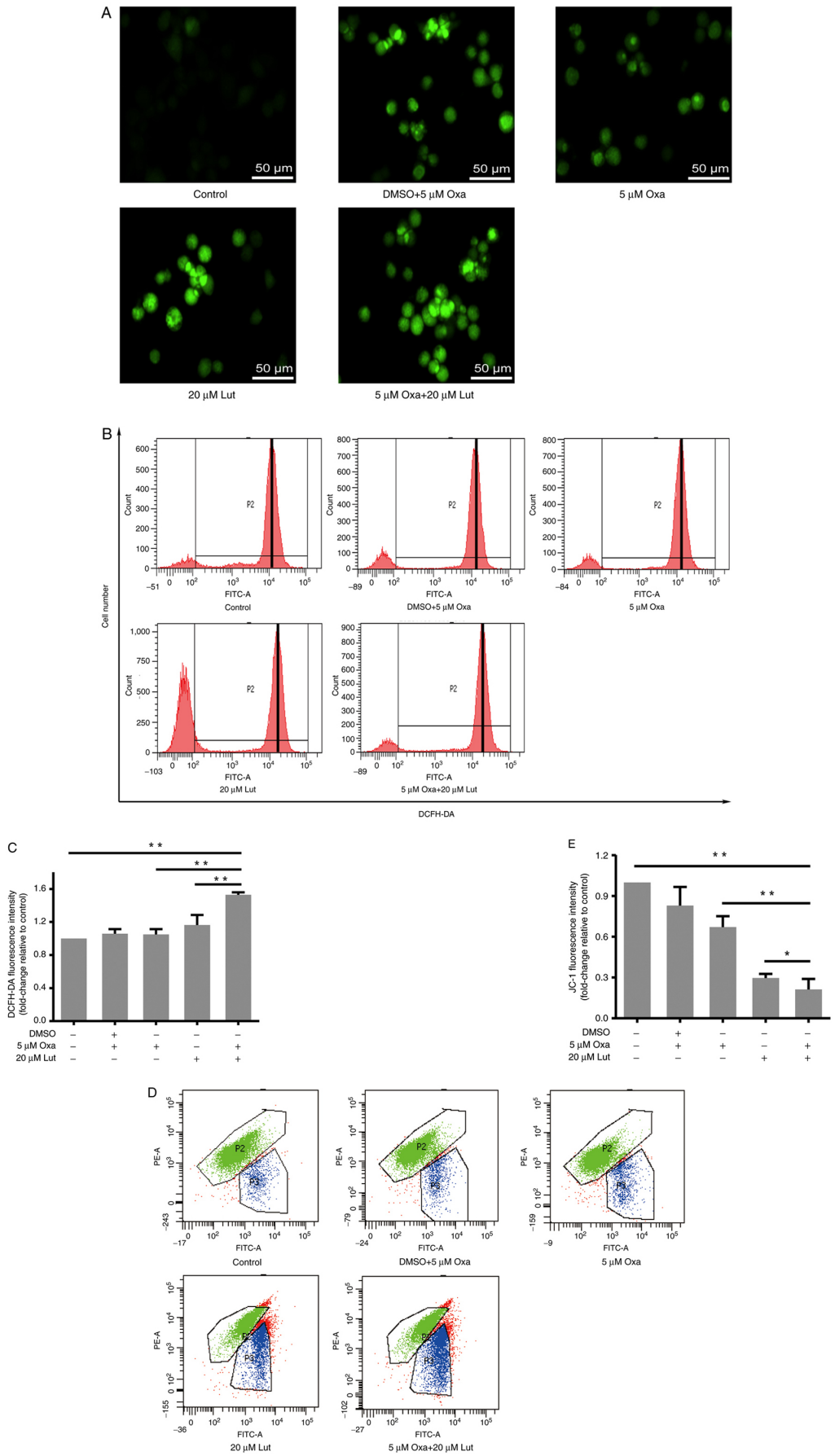

Figure 5. ROS accumulation and mitochondrial membrane potential in mouse forestomach carcinoma cells induced by luteolin (20 μM) and/or oxaliplatin (5 μM). (A) Fluorescence intensity of DCFH-DA was captured under a fluorescence inverted microscope system (magnification, x200). (B and C) ROS levels were analyzed using DCFH-DA staining and flow cytometry. (D and E) Mitochondrial membrane potential was analyzed by JC-1 staining and flow cytometry. *P<0.05, **P<0.01. Experiments were repeated at least in triplicate. Data are presented as mean ± SD. Lut, luteolin; Oxa, oxaliplatin; ROS, reactive oxygen species.

lies in the formation of intrastrand/interstrand DNA cross-links and the impairment of DNA base pairing, replication, and gene transcription (38). Moreover, luteolin is capable of blocking cell cycle development and suppressing cancer cell proliferation by regulating extrinsic and intrinsic signaling pathways (1,39,40). Therefore, it is essential to study the effects of the combined treatment on cell cycle progression in MFC cells. Results of the present study showed that the percentage of cells at G_2/M cell cycle arrest in the combined treatment group was much higher than that in any other treatment group. Binding CDK1 to cyclin B1 is required for the integration of mitochondrial fission with the onset of G_2/M transition (41). Cyclin B1 and CDK1 expression levels were reduced by luteolin and oxaliplatin, suggesting that G_2/M cell cycle arrest played a significant role in inhibiting cancer cell proliferation by luteolin and oxaliplatin. Cell cycle is a highly ordered biological event, which is stringently controlled by cyclins and cyclin-dependent kinases (CDKs). By translocating between cytoplasm and nucleus, cyclin B1/CDK1 is involved in the regulation of the entry into mitosis, nuclear envelope breakdown, and centrosome separation (42). Therefore, the combined treatment with luteolin and oxaliplatin is more likely to suppress the cyclin B1/CDK1 complex expression and to interfere with mitochondrial function, leading to G_2/M cell cycle arrest and apoptosis. The combined treatment induced G_2/M cell cycle arrest by reducing cyclin B1/CDK1, rather by interfering with cyclin A2. In mitotic cell cycles, cyclin A2 begins to accumulate in the S phase and continues to increase from the S phase to late G_2 phase before peaking in early prometaphase (43). The combined treatment with luteolin and oxaliplatin acted on the transition from G_2-M phase, which did not depend on cyclin A2. This suggests that cyclin A2 is not the target of the combined treatment with luteolin and oxaliplatin in MFC cells.

TRAP1, P-ERK1/2, and CDC25C protein expression levels were subsequently assessed. The results showed that they were inhibited by the combined treatment with luteolin and oxaliplatin much more effectively than in any single drug group. Luteolin and oxaliplatin inhibited TRAP1 expression. TRAP1 is a molecular chaperone and belongs to the heat shock protein 90 (Hsp90) family. It is closely related to the occurrence and development of various tumors and is involved in anti-apoptosis and drug resistance, cell cycle progression, cell metabolism, and quality control of specific client proteins (33,44). TRAP1 silencing induces the attenuation of ERK phosphorylation, inhibition of cell cycle progression with cell accumulation in G_0-G_1 and G_2-M transitions, extensive reprogramming of genes involved in cell cycle regulation, and loss of the stem-like signature (2,33). ERK1/2 is involved in the regulation of various cellular processes, including cell proliferation, migration, growth, differentiation, and tumor progression (45). In addition, inactivation of p-ERK1/2 is involved in cell apoptosis induced by pharmacological intervention (46). CDC25C is a novel MAPK ERK1/2 target. ERK1/2 promotes CDC25C ubiquitination and proteasomal degradation, and CDC25C proteolysis is required for sustained G_2 phase arrest (47). It has also been reported that p38MAPK-ERK-JNK signal transduction participates in cell cycle arrest, which has been attributed to nuclear inactivation and degradation of CDC25C (48). The dual-specificity phosphatase CDC25C plays an important role in the regulation of cell cycle progression. CDC25C, as a pivotal upstream regulator of cyclin B1/CDK1, is responsible for the promotion of G_2/M phase transition by triggering CDK1 dephosphorylation to activate the cyclin B1/CDK1 complex (47). CDC25C mainly localizes in the cytoplasm and enters the nucleus to activate the cyclin B1/CDK1 complex before mitosis (48). Results of the western blot analysis revealed that luteolin and oxaliplatin in MFC cells reduced the expression of CDC25C and prevented it from activating the cyclin B1/CDK1 complex, thereby limiting the G_2/M transition and delaying the mitotic process. In addition, it has also been reported that TRAP1 regulates cell cycle arrest by modulating the expression and/or the ubiquitination of key cell cycle regulators, such as CDK1 and cyclin B1. The dual mechanism involves the transcriptional regulation of key proteins and post-transcriptional quality control by inducing the ubiquitination of key proteins enhanced upon TRAP1 downregulation (49). Thus, luteolin and oxaliplatin are more likely to induce TRAP1/ERK1/2/CDC25C downregulation, leading to cyclin B1/CDK1 inhibition, and ultimately triggering G_2/M cell cycle arrest.

Generally, the uncontrolled proliferation of cancer cells is not only related to the disorder of cell cycle progression, but also to the abnormality of apoptosis (50). Therefore, increasing apoptosis is considered as a promising method of cancer treatment. In the present study, the combination of luteolin and oxaliplatin effectively induced apoptosis, much more markedly than the single drug treatments. Therefore, apoptosis may be indispensable to the impact of luteolin and oxaliplatin on inhibiting MFC cell proliferation. Moreover, ROS participates in many biological events, including apoptosis (37). Owing to the structure of phenolic hydroxyl, luteolin may effectively regulate the oxidation-reduction state by interfering with cellular ROS levels (1). Under the combined treatment, ROS significantly increased, and mitochondrial potential significantly decreased, suggesting that the combined treatment damaged mitochondria. ROS levels in cancer cells are normally much higher than those in normal cells; luteolin and oxaliplatin treatment further increased ROS above the steady-state level associated with homeostatic function, which is a lethal threshold for cancer cells (51). More interestingly, oxaliplatin did not effectively exert destructive effects on ROS and the mitochondrial potential; instead, adding luteolin markedly enhanced them, suggesting that the combined treatment with luteolin and oxaliplatin has a different mechanism from the single drug. Previous reports have suggested that the mechanism of anticancer effects of luteolin involves ROS-mediated mitochondrial targeting (52,53). Therefore, a mitochondria-related pathway may participate in the anticancer effects of luteolin and oxaliplatin in MFC cells. Interactions between pro- and anti-apoptotic members of the Bcl-2 protein family highly control mitochondrial outer membrane integrity (54). The expression of Bcl-2 and Bax proteins were interfered by the combined treatment. On intrinsic apoptotic stimuli, such as DNA damage and oxidative stress, Bcl-2 homology 3 (BH3)-only proteins were activated, leading to Bax and Bcl-2 antagonist or killer (BAK) activation and mitochondrial outer membrane permeabilization (MOMP) (55,56). However, the anti-apoptotic protein Bcl-2 could prevent MOMP by binding BH3-only proteins and reversing BAX or BAK activation (55). Therefore, we inferred that the combination treatment may cause MOMP via regulating Bcl-2 and Bax proteins and destroying the integrity of the outer mitochondrial membrane, thereby inducing apoptosis by impairing

mitochondrial membrane potential and ROS balance. Notably, cyclin B1/CDK1 is pivotal in regulating mitochondrial metabolism in tumors. Among all the subunits of mitochondrial respiration chain (complex I-V), 12 subunits, including eight complex I subunits (NADH ubiquinone oxidoreductase), can be potentially phosphorylated by cyclin B1/CDK1, indicating that cyclin B1/CDK1 is involved in controlling ATP output and triggering ROS generation (41,57).

In conclusion, luteolin and oxaliplatin exerted synergistic effects in inhibiting MFC cell proliferation by inducing G_2/M cell cycle arrest and apoptosis. Inhibition of the TRAP1/P-ERK1/2/CDC25C/CDK1/cyclin B1 pathway was indispensable to the induction of G_2/M cell cycle arrest. In addition, the combined therapy significantly interfered with oxidative balance and MMP, and regulated Bax and Bcl-2 protein expression levels, thereby leading to apoptosis. Therefore, our findings indicated that luteolin potentiated low-dose oxaliplatin-induced inhibitory effects on proliferation in MFC cells. Findings of the present study may therefore provide the theoretical basis for the use of luteolin in clinical practice in the future.

Acknowledgements

Not applicable.

Funding

This study was supported by the National Natural Science Foundation of China (grant no. 31471338), the Key Research and Development Program of Shandong Province of China (grant no. 2019GSF108214) and the Natural Science Foundation of Shandong Province (grant no. ZR2016HB51).

Availablity of data and materials

The datasets used and/or analyzed during the current study are available from the corresponding author on reasonable request.

Authors' contributions

JM conceived the experiments and was responsible for writing the manuscript. JM and XC conducted and completed the experiments. XZ and ZP interpreted and analyzed the data. DL and WH were responsible for data interpretation and revised the final version of the manuscript. QZ and XT participated into study design and provided funding. JM and XC confirm the authenticity of all the raw data. All authors have read and approved the final manuscript.

Ethics approval and consent to participate

Not applicable.

Patient consent for publication

Not applicable.

Competing interests

The authors declare that they have no competing interests.

References

1. Imran M, Rauf A, Abu-Izneid T, Nadeem M, Shariati MA, Khan IA, Imran A, Orhan IE, Rizwan M, Atif M, *et al*: Luteolin, a flavonoid, as an anticancer agent: A review. Biomed Pharmacother 112: 108612, 2019.
2. Lettini G, Maddalena F, Sisinni L, Condelli V, Matassa DS, Costi MP, Simoni D, Esposito F and Landriscina M: TRAP1: A viable therapeutic target for future cancer treatments? Expert Opin Ther Targets 21: 805-815, 2017.
3. Limagne E, Thibaudin M, Nuttin L, Spill A, Derangère V, Fumet JD, Amellal N, Peranzoni E, Cattan V and Ghiringhelli F: Trifluridine/tipiracil plus oxaliplatin improves PD-1 blockade in colorectal cancer by inducing immunogenic cell death and depleting macrophages. Cancer Immunol Res 7: 1958-1969, 2019.
4. Patel TH and Cecchini M: Targeted therapies in advanced gastric cancer. Curr Treat Options Oncol 21: 70, 2020.
5. Wei TT, Lin YT, Tang SP, Luo CK, Tsai CT, Shun CT and Chen CC: Metabolic targeting of HIF-1α potentiates the therapeutic efficacy of oxaliplatin in colorectal cancer. Oncogene 39: 414-427, 2020.
6. Fujita S, Hirota T, Sakiyama R, Baba M and Ieiri I: Identification of drug transporters contributing to oxaliplatin-induced peripheral neuropathy. J Neurochem 148: 373-385, 2019.
7. Cao P, Xia Y, He W, Zhang T, Hong L, Zheng P, Shen X, Liang G, Cui R and Zou P: Enhancement of oxaliplatin-induced colon cancer cell apoptosis by alantolactone, a natural product inducer of ROS. Int J Biol Sci 15: 1676-1684, 2019.
8. Riddell IA: Cisplatin and oxaliplatin: Our current understanding of their actions. Met Ions Life Sci 18, 2018.
9. Stankovic JSK, Selakovic D, Mihailovic V and Rosic G: Antioxidant supplementation in the treatment of neurotoxicity induced by platinum-based chemotherapeutics - a review. Int J Mol Sci 21: 7753, 2020.
10. Cao LX, Chen ZQ, Jiang Z, Chen QC, Fan XH, Xia SJ, Lin JX, Gan HC, Wang T and Huang YX: Rapid rehabilitation technique with integrated traditional Chinese and Western medicine promotes postoperative gastrointestinal function recovery. World J Gastroenterol 26: 3271-3282, 2020.
11. Lee YC, Chen YH, Huang YC, Lee YF and Tsai MY: Effectiveness of combined treatment with traditional Chinese medicine and Western medicine on the prognosis of patients with breast cancer. J Altern Complement Med 26: 833-840, 2020.
12. Tang WR, Yang SH, Yu CT, Wang CC, Huang ST, Huang TH, Chiang MC and Chang YC: Long-term effectiveness of combined treatment with traditional Chinese medicine and Western medicine on the prognosis of patients with lung cancer. J Altern Complement Med 22: 212-222, 2016.
13. Martinez-Torres AC, Reyes-Ruiz A, Benítez-Londoño M, Franco-MolinaMAandRodriguez-PadillaC:IMMUNEPOTENT CRP induces cell cycle arrest and caspase-independent regulated cell death in HeLa cells through reactive oxygen species production. BMC Cancer 18: 13, 2018.
14. Ren B, Ye L, Gong J, Ren H, Ding Y, Chen X, Liu X, Lu P, Wei F, Xu W, *et al*: Alteronol enhances the anti-tumor activity and reduces the toxicity of high-dose adriamycin in breast cancer. Front Pharmacol 10: 285, 2019.
15. Pu Y, Zhang T, Wang J, Mao Z, Duan B, Long Y, Xue F, Liu D, Liu S and Gao Z: Luteolin exerts an anticancer effect on gastric cancer cells through multiple signaling pathways and regulating miRNAs. J Cancer 9: 3669-3675, 2018.
16. Xu J, Xu H, Yu Y, He Y, Liu Q and Yang B: Combination of luteolin and solifenacin improves urinary dysfunction induced by diabetic cystopathy in rats. Med Sci Monitor 24: 1441-1448, 2018.
17. Park S, Kim DS, Kang S and Kim HJ: The combination of luteolin and l-theanine improved Alzheimer disease-like symptoms by potentiating hippocampal insulin signaling and decreasing neuroinflammation and norepinephrine degradation in amyloid-β-infused rats. Nutr Res 60: 116-131, 2018.
18. Hashemzaei M, Abdollahzadeh M, Iranshahi M, Golmakani E, Rezaee R and Tabrizian K: Effects of luteolin and luteolin-morphine co-administration on acute and chronic pain and sciatic nerve ligated-induced neuropathy in mice. J Complement Integr Med 14, 2017.
19. Chakrabarti M and Ray SK: Anti-tumor activities of luteolin and silibinin in glioblastoma cells: Overexpression of miR-7-1-3p augmented luteolin and silibinin to inhibit autophagy and induce apoptosis in glioblastoma in vivo. Apoptosis 21: 312-328, 2016.

20. Feng XQ, Rong LW, Wang RX, Zheng XL, Zhang L, Zhang L, Lin Y, Wang X and Li ZP: Luteolin and sorafenib combination kills human hepatocellular carcinoma cells through apoptosis potentiation and JNK activation. Oncol Lett 16: 648-653, 2018.
21. Soliman NA, Abd-Ellatif RN, ELSaadany AA, Shalaby SM and Bedeer AE: Luteolin and 5-flurouracil act synergistically to induce cellular weapons in experimentally induced solid ehrlich carcinoma: Realistic role of P53; a guardian fights in a cellular battle. Chem Biol Interact 310: 108740, 2019.
22. Zhu Y, Liu R, Shen Z and Cai G: Combination of luteolin and lycopene effectively protect against the 'two-hit' in NAFLD through Sirt1/AMPK signal pathway. Life Sci 256: 117990, 2020.
23. Zhang HH and Guo XL: Combinational strategies of metformin and chemotherapy in cancers. Cancer Chemother Pharmacol 78: 13-26, 2016.
24. Zhao XQ, Tang H, Yang J, Gu XY, Wang SM and Ding Y: MicroRNA-15a-5p down-regulation inhibits cervical cancer by targeting TP53INP1 in vitro. Eur Rev Med Pharmacol Sci 23: 8219-8229, 2019.
25. Chou TC: Drug combination studies and their synergy quantification using the Chou-Talalay method. Cancer Res 70: 440-446, 2010.
26. Bressy C, Droby GN, Maldonado BD, Steuerwald N and Grdzelishvili VZ: Cell cycle arrest in G_2/M phase enhances replication of interferon-sensitive cytoplasmic RNA viruses via inhibition of antiviral gene expression. J Virol 93: e01885-18, 2019.
27. Gong Y, Luo S, Fan P, Zhu H, Li Y and Huang W: Growth hormone activates PI3K/Akt signaling and inhibits ROS accumulation and apoptosis in granulosa cells of patients with polycystic ovary syndrome. Reprod Biol Endocrinol 18: 121, 2020.
28. Zhang X, Qin Y, Pan Z, Li M, Liu X, Chen X, Qu G, Zhou L, Xu M, Zheng Q and Li D: Cannabidiol induces cell cycle arrest and cell apoptosis in human gastric cancer SGC-7901 cells. Biomolecules 9: 302, 2019.
29. Si L, Yan X, Wang Y, Ren B, Ren H, Ding Y, Zheng Q, Li D and Liu Y: Chamaejasmin B decreases malignant characteristics of mouse melanoma B16F0 and B16F10 cells. Front Oncol 10: 415, 2020.
30. Hu X, Yang Z, Liu W, Pan Z, Zhang X, Li M, Liu X, Zheng Q and Li D: The anti-tumor effects of p-coumaric acid on melanoma A375 and B16 cells. Front Oncol 10: 558414, 2020.
31. Choi YH: Isorhamnetin induces ROS-dependent cycle arrest at G2/M phase and apoptosis in human hepatocarcinoma Hep3B cells. Gen Physiol Biophys 38: 473-484, 2019.
32. Iida K, Naiki T, Naiki-Ito A, Suzuki S, Kato H, Nozaki S, Nagai T, Etani T, Nagayasu Y, Ando R, *et al*: Luteolin suppresses bladder cancer growth via regulation of mechanistic target of rapamycin pathway. Cancer Sci 111: 1165-1179, 2020.
33. Palladino G, Notarangelo T, Pannone G, Piscazzi A, Lamacchia O, Sisinni L, Spagnoletti G, Toti P, Santoro A, Storto G, *et al*: TRAP1 regulates cell cycle and apoptosis in thyroid carcinoma cells. Endocr Relat Cancer 23: 699-709, 2016.
34. Xie S, Wang X, Gan S, Tang X, Kang X and Zhu S: The mitochondrial chaperone TRAP1 as a candidate target of oncotherapy. Front Oncol 10: 585047, 2020.
35. Obeng E: Apoptosis (programmed cell death) and its signals-a review. Braz J Biol 81: 1133-1143, 2021.
36. Pistritto G, Trisciuoglio D, Ceci C, Garufi A and D'Orazi G: Apoptosis as anticancer mechanism: Function and dysfunction of its modulators and targeted therapeutic strategies. Aging (Albany NY) 8: 603-619, 2016.
37. Yang Y, Karakhanova S, Hartwig W, D'Haese JG, Philippov PP, Werner J and Bazhin AV: Mitochondria and mitochondrial ROS in cancer: Novel targets for anticancer therapy. J Cell Physiol 231: 2570-2581, 2016.
38. Rogers BB, Cuddahy T, Briscella C, Ross N, Olszanski AJ and Denlinger CS: Oxaliplatin: Detection and management of hypersensitivity reactions. Clin J Oncol Nurs 23: 68-75, 2019.
39. Chen ZC, Zhang B, Gao F and Shi RJ: Modulation of G_2/M cell cycle arrest and apoptosis by luteolin in human colon cancer cells and xenografts. Oncol Lett 15: 1559-1565, 2018.
40. Anson DM, Wilcox RM, Huseman ED, Stump TA, Paris RL, Darkwah BO, Lin S, Adegoke AO, Gryka RJ, Jean-Louis DS and Amos S: Luteolin decreases epidermal growth factor receptor-mediated cell proliferation and induces apoptosis in glioblastoma cell lines. Basic Clin Pharmacol 123: 678-686, 2018.
41. Xie BW, Wang SY, Jiang N and Li JJ: Cyclin B1/CDK1-regulated mitochondrial bioenergetics in cell cycle progression and tumor resistance. Cancer Lett 443: 56-66, 2019.
42. Wang ZQ, Fan M, Candas D, Zhang TQ, Qin L, Eldridge A, Wachsmann-Hogiu S, Ahmed KM, Chromy BA, Nantajit D, *et al*: Cyclin B1/Cdk1 coordinates mitochondrial respiration for cell-cycle G2/M progression. Dev Cell 29: 217-232, 2014.
43. Silva Cascales H, Burdova K, Middleton A, Kuzin V, Müllers E, Stoy H, Baranello L, Macurek L and Lindqvist A: Cyclin A2 localises in the cytoplasm at the S/G2 transition to activate PLK1. Life Sci Alliance 4: e202000980, 2021.
44. Li XT, Li YS, Shi ZY and Guo XL: New insights into molecular chaperone TRAP1 as a feasible target for future cancer treatments. Life Sci 254: 117737, 2020.
45. Shingyochi Y, Kanazawa S, Tajima S, Tanaka R, Mizuno H and Tobita M: A low-level carbon dioxide laser promotes fibroblast proliferation and migration through activation of Akt, ERK, and JNK. PLoS One 12: e0168937, 2017.
46. Liu L, Xing YH, Cao MY, Xu JL and Chen JJ: Exogenous NO induces apoptosis of hepatocellular carcinoma cells via positive p38/JNK signaling pathway and negative ERK signaling pathways. Mol Cell Biochem 476: 1651-1661, 2021.
47. Liu K, Zheng M, Lu R, Du J, Zhao Q, Li Z, Li Y and Zhang S: The role of CDC25C in cell cycle regulation and clinical cancer therapy: A systematic review. Cancer Cell Int 20: 213, 2020.
48. Liu K, Lu R, Zhao Q, Du J, Li Y, Zheng M and Zhang S: Association and clinicopathologic significance of p38MAPK-ERK-JNK-CDC25C with polyploid giant cancer cell formation. Med Oncol 37: 6, 2020.
49. Sisinni L, Maddalena F, Condelli V, Pannone G, Simeon V, Li Bergolis V, Lopes E, Piscazzi A, Matassa DS, Mazzoccoli C, *et al*: TRAP1 controls cell cycle G2-M transition through the regulation of CDK1 and MAD2 expression/ubiquitination. J Pathol 243: 123-134, 2017.
50. Kinnaird A and Michelakis ED: Metabolic modulation of cancer: A new frontier with great translational potential. J Mol Med (Berl) 93: 127-142, 2015.
51. Hirata T, Cho YM, Suzuki I, Toyoda T, Akagi JI, Nakamura Y, Numazawa S and Ogawa K: 4-Methylthio-3-butenyl isothiocyanate (MTBITC) induced apoptotic cell death and G2/M cell cycle arrest via ROS production in human esophageal epithelial cancer cells. J Toxicol Sci 44: 73-81, 2019.
52. Seydi E, Salimi A, Rasekh HR, Mohsenifar Z and Pourahmad J: Selective cytotoxicity of luteolin and kaempferol on cancerous hepatocytes obtained from rat model of hepatocellular carcinoma: Involvement of ROS-mediated mitochondrial targeting. Nutr Cancer 70: 594-604, 2018.
53. Wang Q, Wang H, Jia Y, Pan H and Ding H: Luteolin induces apoptosis by ROS/ER stress and mitochondrial dysfunction in gliomablastoma. Cancer Chemother Pharmacol 79: 1031-1041, 2017.
54. Tait SW and Green DR: Mitochondria and cell death: Outer membrane permeabilization and beyond. Nat Rev Mol Cell Biol 11: 621-632, 2010.
55. Peña-Blanco A and García-Sáez AJ: Bax, Bak and beyond-mitochondrial performance in apoptosis. FEBS J 285: 416-431, 2018.
56. Flores-Romero H, Ros U and Garcia-Saez AJ: Pore formation in regulated cell death. FEBS J 39: e105753, 2020.
57. Shendge AK, Chaudhuri D and Mandal N: The natural flavones, acacetin and apigenin, induce Cdk-Cyclin mediated G2/M phase arrest and trigger ROS-mediated apoptosis in glioblastoma cells. Mol Biol Rep 48: 539-549, 2021.